



Tidal-to-seasonal variability in the parameters of the carbonate system in a shallow tidal creek influenced by anthropogenic inputs, Rio San Pedro (SW Iberian Peninsula)

Mercedes de la Paz*, Abelardo Gómez-Parra, Jesús Forja

Departamento de Química-Física, Facultad de Ciencias del Mar y Ambientales, Universidad de Cádiz, Campus Río San Pedro s/n, Puerto Real, Cádiz 11510, Spain

ARTICLE INFO

Article history:

Received 3 October 2007

Received in revised form

31 March 2008

Accepted 2 April 2008

Available online 7 April 2008

Keywords:

Inorganic carbon

Tidal creeks

Temporal variability

DIC export

Rio San Pedro

Bay of Cadiz

ABSTRACT

The main objective of the present study is to assess the temporal variability of the carbonate system, and the mechanisms driving that variability, in the Rio San Pedro, a tidal creek located in the Bay of Cadiz (SW Iberian Peninsula). This shallow tidal creek is affected by effluents of organic matter and nutrients from surrounding marine fish farms. In 2004, 11 tidal samplings, seasonally distributed, were carried out for the measurement of total alkalinity (TA), pH, dissolved oxygen and Chlorophyll-*a* (Chl-*a*) using a fixed station. In addition, several longitudinal samplings were carried out both in the tidal creek and in the adjacent waters of the Bay of Cadiz, in order to obtain a spatial distribution of the carbonate parameters. Tidal mixing is the main factor controlling the dissolved inorganic carbon (DIC) variability, showing almost conservative behaviour on a tidal time scale. The amplitude of the daily oscillations of DIC, pH and chlorophyll show a high dependence on the spring-neap tide sequence, with the maximum amplitude associated with spring tides. Additionally, a marked seasonality has been found in the DIC, pH and oxygen concentrations. This seasonality seems to be related to the increase in metabolic rates with the temperature, the alternation of storm events and high evaporation rates, together with intense seasonal variability in the discharges from fish farms. In addition, the export of DIC from the Rio San Pedro to the adjacent coastal area has been evaluated using the tidal prism model, obtaining a net export of $1.05 \times 10^{10} \text{ g C yr}^{-1}$.

© 2008 Elsevier Ltd. All rights reserved.

1. Introduction

Coastal environments represent important pathways between land and the open ocean. They play a significant role in modifying the flows of matter and energy between these two systems. During the last century, the coastal ocean has been exposed to large perturbations, mostly related to human activities on land. Prolonged and intensive use of inorganic fertilisers in agriculture, changes in land use pattern, and discharge of industrial and urban waste have all contributed to the eutrophication not only of river water but also of coastal ocean waters on a global scale. Over the past 50 years, the fluxes of natural and synthetic materials from the terrestrial environment to the coastal ocean have increased by a factor of 1.5–2 because of human-induced perturbations (Meybeck and Ragu, 1995). However, it is expected that the natural control mechanisms in the coastal ocean will serve to reduce and perhaps eliminate the effect of the perturbation within

a relatively short period, and that these mechanisms are efficient enough to prevent the accumulation of “pollutants” and their byproducts (Rabouille et al., 2001). Therefore, the synthesis of data on input, burial, and oxidation of organic matter, and organic carbon metabolism is critical for developing coastal ocean carbon budgets (Smith and Hollibaugh, 1993).

The Bay of Cadiz is becoming a focal point for intensive and extensive aquaculture in former salt marsh areas. The risk of negative environmental impact associated with this development has been identified (Alongi, 2002). Previously, attention has been focused on discharges of nutrients and organic matter, but to date, only a limited number of studies are available concerning the inorganic carbon evolution in these systems.

Previous studies have been undertaken in pristine systems such as in the temperate regions of the south-eastern United States along the coast of Georgia, a coastal area also largely dominated by salt marshes (Cai and Wang, 1998; Cai et al., 1999). High rates of respiration in the sediments of intertidal marshes, and transport of DIC from marshes to estuaries during the tidal cycle are thought to be the primary controls on carbon and oxygen dynamics that create a net heterotrophy of the system (Cai et al., 1999). However, few studies have been carried out in Europe on

* Corresponding author. Present address: Instituto de Investigaciones Marinas, CSIC, Eduardo Cabello 6, 36208 Vigo, Spain. Tel.: +34 956 01 67 41; fax: +34 956 01 60 40.

E-mail address: mercedes.delapaz@uca.es (M. de la Paz).

the complex salt marshes–tidal creek system and the impacts of human activities on them, for the purposes of quantifying diurnal and seasonal variations in carbon and oxygen system parameters by means of direct measurements.

We report results from the *in situ* measurement of carbonate system parameters, from tidal to seasonal scales, in the Rio San Pedro tidal creek, a shallow system in the SW of the Iberian Peninsula that is highly affected by terrestrial and anthropogenic inputs.

2. Material and methods

2.1. Study site

The Rio San Pedro is a tidal creek located in the Southwest of the Iberian Peninsula (Fig. 1). Originally, it was a distributary of the Guadalete River, but it was artificially blocked 12 km from the river mouth during the 1960s. Tidal exchange is usually the primary driving force for interactions between the tidal creek and the Bay of Cadiz. The Rio San Pedro is subject to a semi-diurnal tidal regime with the height of the tidal column varying from 3.5 m at spring tide to 0.5 m at neap tide; the tidal creek has an average overall depth of between 3 and 5 m. The water column is well mixed with no significant differences between surface and bottom (González-Gordillo et al., 2003). The main content of the Rio San Pedro is seawater except for occasional freshwater inputs from rainfall and land drainage inputs. The Bay of Cadiz is surrounded by a broad area of salt marshes subject to severe human pressure from increasing population density, as well as from the aquaculture and other industries discharging into the Bay and the salt marsh inlets. Although the landscape surrounding

the Rio San Pedro was originally formed by an extensive area of salt marshes, progressive exploitation by the human population, such as salt marsh desiccation by blockage, fish farm construction, salt production factories, and other human activities, has significantly reduced the proportion of the area remaining as natural marsh. The actual channel of the Rio San Pedro is effectively isolated, laterally by mean of an embankment that separates the channel from the various industries that exploit the salt marsh environment, and the more inland reaches of the creek are restricted by a dam, which allows some water exchange between the upper salt marshes area and the tidal creek at times of very high water level. This human-made separation suggests that the influence of the salt marsh on the Rio San Pedro is only moderate. There is a fish farm located at the head of the creek. Tovar et al. (2000a) determined the loading of large quantities of dissolved nutrients, organic matter and suspended solids in the effluents of the marine fish farm, which is dedicated to the intensive culture of gilthead seabream (*Sparus aurata*). It was estimated that 9105 kg of suspended solids, 843 kg of particulate organic matter (POM), 36 kg of N-NH_4^+ , 5 kg of N-NO_2^- , 7 kg of N-NO_3^- and 3 kg of P-PO_4^{3-} dissolved in saline water were discharged to the Rio San Pedro for each tonne of fish cultivated. The mean annual production of this fish farm is around 10^6 kg. The total extension of the fish farm is about 1.3 km², where approximately 80% is occupied by a series of pools excavated in the sandy soil, with an average depth of 1 m (Tovar et al., 2000a). There are two pumping stations for providing water from the tidal creek to the fish farm, and a single discharge point located around 10 km from the mouth of the creek. Daily, a volume of water of 240,000 m³ (Tovar et al., 2000a) is exchanged with the tidal creek, this represents 8% of the tidal prism volume exchanged between the Rio San Pedro and the Bay of Cadiz.

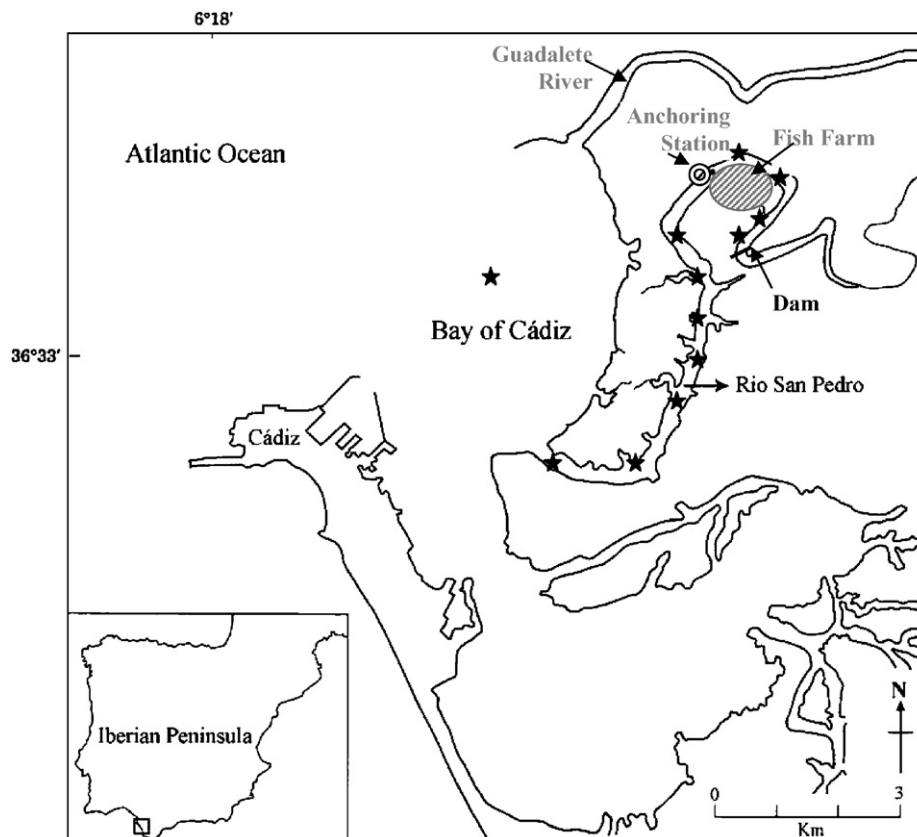


Fig. 1. Location of the sampling stations along the Rio San Pedro. Longitudinal sampling stations are indicated as black stars.

2.2. Samplings and methods

Several sampling strategies were carried out in order to characterise the temporal and spatial variability of the physico-chemical properties in the Rio San Pedro and the adjacent Bay of Cadiz. To study the spatial gradient inside the tidal creek, two longitudinal samplings were carried out at 12 stations, extending from the mouth of the creek to the upstream dam, on 4 June and 30 September 2003. Another two sampling campaigns were performed in the Bay of Cadiz, from on board the R/V *Mytilus*, to compare the characteristics of the salt marshes with those of more open coastal waters, in June 2003 and February 2006, as the two seasonal extremes. In addition, 11 tidal samplings were carried out at a fixed station located inside the tidal creek (see Fig. 1). Tidal samplings were seasonally distributed basically over 4 months covering a spring, neap and intermediate tide for each month (see Table 1); those done in February/March and April/May lasted 24 h for some of the variables—total alkalinity (TA), dissolved inorganic carbon (DIC), salinity and temperature, whereas the July and September samplings lasted 12–14 h. All the sampling locations are indicated in Fig. 1. Based on the seasonal temperature cycle, in this work seasons are defined as: winter (December–February), spring (March–May), summer (June–August) and autumn (September–November).

Subsurface water samples were taken in most of the samplings, continuously for temperature and salinity, and discretely for total alkalinity (TA), pH, Chlorophyll-*a* (Chl-*a*) and dissolved oxygen (DO). Salinity and temperature were continuously recorded using a SeaBird thermosalinometer (SBD-45-MicroTSG) to which the water was supplied by an underway pump. The pH was measured using a glass-combined electrode (Methrom) calibrated in the free pH scale (Zeebe and Wolf-Gladrow, 2001). The alkalinity computation was made from the titration curve by means of the Gran Function and taking into account the correction for sulphate and fluoride interaction, using the constants proposed by Dickson (1990) and by Dickson and Riley (1979), respectively. The DIC concentration was computed from TA and pH, using the K1 and K2 acidity constants proposed by Lueker et al. (2000) in the total pH scale. The TA measurements were validated with reference standards obtained from A. Dickson (Scripps Institute of Oceanography, San Diego, USA) to an accuracy of $\pm 2 \mu\text{mol kg}^{-1}$.

The continuous surface water fCO₂ measurements in the Bay of Cadiz were performed using the equilibration technique. The equilibration processes were a mixture of laminar-flow and a bubble type connected to an infrared analyser (Li-Cor 6262) in accordance with the system detailed described in Körtzinger et al. (1996).

The samples for DO were fixed in a sealed flask and stored in darkness for 24 h as described by the Winkler method, for later analysis by potentiometric titration (Metrohm 670 Titroprocessor). The apparent oxygen utilisation (AOU) is defined as the deviation of oxygen from a DO concentration in equilibrium with the atmosphere calculated from the Benson and Krause (1984) solubility equation. Chl-*a* was determined in a glass fibre filter by fluorescence after extraction in 90% acetone (Turner Designs 10-AU). Suspended particulate matter (SPM) was determined in 500 mL of filtered water sampled following the methodology proposed by APHA (1992).

3. Results and discussion

3.1. Spatial variability

Fig. 2 represents the longitudinal gradient for salinity, SPM, DIC and pH in the Rio San Pedro tidal creek measured in June and September. The salinity increases toward the inner extreme of the creek due to lower flushing rates and evaporation processes. There exists a pronounced spatial gradient for the SPM, DIC and pH as a result of the impact of the aquaculture activities, the outflow from which is located around 10 km upstream from the mouth of the creek. The SPM concentrations range from 10.8 mgL^{-1} at the mouth of the creek to 57.9 mgL^{-1} close to the wastewater discharge point. The DIC presents a maximum of $3240 \pm 20 \mu\text{mol kg}^{-1}$ at the location of the wastewater discharge point and decreases almost linearly towards the mouth where the minimum concentration is $2560 \pm 12 \mu\text{mol kg}^{-1}$. Higher DIC and SPM values are observed in September than in June. This agrees with a higher activity of the fish farm in September (Tovar et al., 2000b). The pH follows a similar longitudinal pattern, presenting a relatively acidic value (7.40 ± 0.01) at the fish farm effluent discharge point and increasing towards the creek mouth to 7.83 ± 0.03 . Tovar et al. (2000a) studied the longitudinal distribution of various physico-chemical properties in the Rio San Pedro, and suggested that the low pH values in the fish farm effluent are due to the high ammonium concentration and to the acidic character of the faeces and fish food. Additionally, the large amounts of suspended solids present are potentially one of the most serious environmental problems caused by aquaculture due to the decreased availability of light in the water and the inputs of organic particulate matter.

The comparison of the physico-chemical parameters between the Bay of Cadiz and the Rio San Pedro helps in assessing the magnitudes of the various different processes taking place in the Rio San Pedro. Considerable differences in concentrations

Table 1

Results from the tidal samplings in the Rio San Pedro for salinity, temperature, TA, DIC, pH, AOU, Chl-*a* and water renewal (%) values

Date (2004)	Salinity	Temperature (°C)	TA ($\mu\text{mol kg}^{-1}$)	DIC ($\mu\text{mol kg}^{-1}$)	pH	AOU ($\mu\text{mol kg}^{-1}$)	Chl- <i>a</i> ($\mu\text{g L}^{-1}$)	% water renewal
16 February (medium)	30.1–33.5	14.8–16.5	2862–3148	2792–3096	7.54–7.73	3.2–32.6	0.8–4.5	28
19 February (spring)	30.6–35.3	13.5–15.0	2540–3144	2404–3115	7.53–7.84	9.1–49.4	1.4–2.1	43
01 March (neap)	20.2–25.7	12.5–15.2	2810–3116	2760–3035	7.57–7.78	–27.8–39.6	1.9–14.5	18
27 April (neap)	33.1–34.8	18.9–21.6	2570–2867	2480–2767	7.51–7.87	–16.7–33.1	1.0–6.3	16
04 May (spring)	32.2–33.9	16.9–18.95	2610–3037	2390–2918	7.57–7.99	10.1–64.4	1.1–2.8	49
19 May (medium)	32.7–35.1	18.4–20.3	2750–3310	2550–3179	7.61–8.16	10.7–33.0	1.2–2.5	41
01 July (spring)	36.9–39.8	26.1–28.1	2560–3075	2330–2960	7.48–7.84	20.5–120.5	3.1–9.1	43
12 July (neap)	38.4–40.4	25.6–27.3	2830–3165	2710–3112	7.31–7.59	26.6–63.5	1.1–5.7	24
26 July (medium)	38.4–40.6	29–31.4	2800–3126	2690–3086	7.31–7.80	32.4–67.5	1.5–7.8	30
07 September (neap)	37.8–39.2	24.5–26.1	2830–3146	2740–3114	7.37–7.58	17.8–49.8	1.6–6.5	16
15 September (spring)	35.7–39.3	23.4–24.1	2550–3129	2330–3072	7.42–7.89	–8.6–128.7	1.7–5.8	46

Spring–neap tidal cycle has been also included for each sampling date.

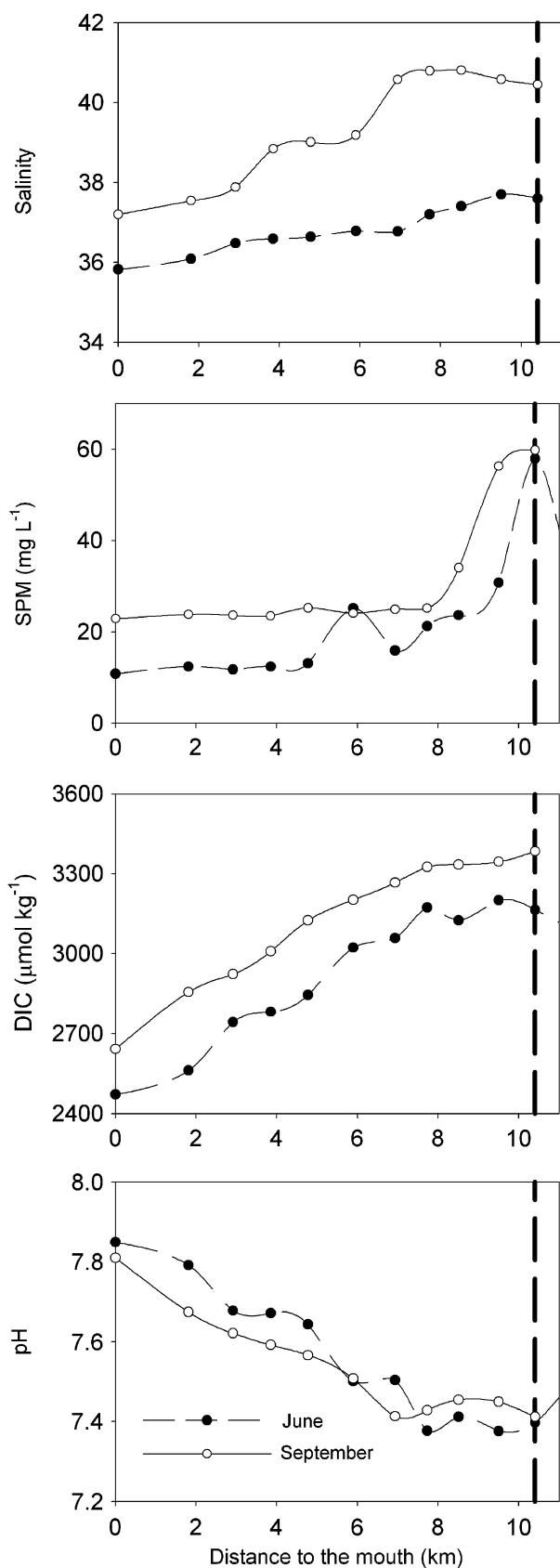


Fig. 2. Longitudinal concentration gradients of suspended particulate matter (SPM), salinity, dissolved inorganic carbon (DIC) and pH along the Rio San Pedro. Locations of the sampling stations are described in Fig. 1. The site of the fish farm discharge point is marked by the vertical broken line.

between the Rio San Pedro and the Bay of Cadiz were recorded. Two sets of data obtained in February and June in a sampled area in the Bay of Cadiz are presented as an example of the relative spatial heterogeneity in the values of the salinity and $f\text{CO}_2$ in the Bay compared to the values found in the Rio San Pedro (Fig. 3). In February, the salinity is lower but increases with the distance from the coastline in February due to the rainwater and land drainage inputs, with an average value of 35.54 ± 0.33 , whereas in June the absence of significance freshwater inputs and increased evaporation rate gives a higher average salinity value of 36.67 ± 0.07 . Regarding the $f\text{CO}_2$ values, the average concentration ranges from $382 \pm 10 \mu\text{atm}$ in February to $443 \pm 27 \mu\text{atm}$ in June. It is notable that there is a change from CO_2 undersaturation to oversaturation from winter to summer due to the seasonal changes in temperature ($14.6\text{--}24.2^\circ\text{C}$). In order to assess the mechanisms driving $f\text{CO}_2$ other than temperature, the $f\text{CO}_2$ database has been normalised to a theoretical average temperature of 20°C , using the expression proposed by Takahashi et al. (1993). Henceforth in this paper, this normalised $f\text{CO}_2$ will be referred to as $f\text{CO}_2@20^\circ\text{C}$. The average $f\text{CO}_2@20^\circ\text{C}$ for February is $499 \pm 15 \mu\text{atm}$ while in June its averaged value is $374 \pm 23 \mu\text{atm}$. These values lead us to consider the temperature to be the mechanism that controls the role of the Bay of Cadiz as either a sink or a source of CO_2 to the atmosphere. Additionally, the higher values for the $f\text{CO}_2@20^\circ\text{C}$ linked to the lower salinity observed in February can be explained by terrestrial inputs originated from the on-land run-off, whereas in June, the lower $f\text{CO}_2@20^\circ\text{C}$ can be explained by primary production being favoured over respiration; this is consistent with the negative AOU observed.

In the Bay the $f\text{CO}_2$ variability in June is twice that observed in February but this is insignificant compared to the seasonal variability for $f\text{CO}_2$ found inside the Rio San Pedro tidal creek (at the anchoring station) where the $f\text{CO}_2$ values ranges from 380 in February to $3760 \mu\text{atm}$ in July.

The DIC concentration in the Bay of Cadiz varies between $2125 \pm 28 \mu\text{mol kg}^{-1}$ in February and $2311 \pm 20 \mu\text{mol kg}^{-1}$ in June. The AOU ranges from $0.7 \pm 20 \mu\text{mol kg}^{-1}$ in February to $-15.5 \pm 13 \mu\text{mol kg}^{-1}$ in June.

3.2. Temporal variability

Hydrochemical monitoring of tidal cycles seasonally distributed throughout the year allows the analysis of the effects of seasonal and daily fluctuations, as well as evaluation of the effects of the spring–neap tidal sequence.

3.2.1. Tidal (diurnal) variability

As an example, a set of tidal variations of temperature, salinity, DIC, TA, pH, Chl-*a* and AOU are depicted in Fig. 4; the range of concentrations and values measured for each tidal cycle are summarised in Table 1. High temporal variability is found for all the variables during the tidal cycle. The common tendency is that salinity tracks the tidal mixing with two maxima and two minima per day. Winter conditions are characterised by discrete precipitation, storms and land drainage inputs making the water in the estuary fresher than the water of the Bay of Cadiz; thus, the salinity shows a peak at high tide. The summer situation is characterised by total absence of freshwater inputs and the high temperatures and evaporation rates reached; as a result, the creek water is saltier than the water of the Bay of Cadiz, and shows a salinity maximum at low tide. The daily temperature variability is related more to the solar insolation rather than to tidal mixing, as can be noted from the 24 h samplings (February and May).

DIC and TA show maximum concentration at low tide and minimum at high tide throughout the year. The amplitude of the

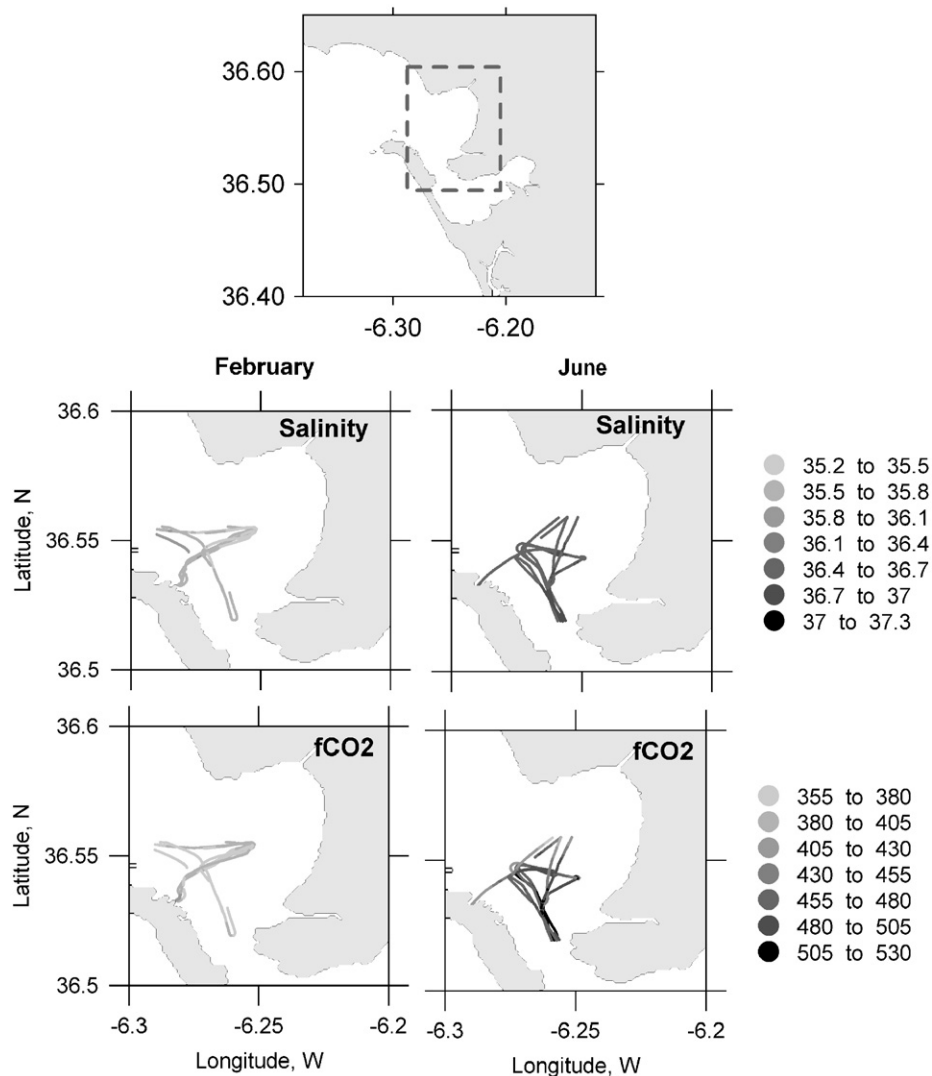


Fig. 3. Spatial variability of salinity and CO₂ fugacity in the Bay of Cadiz, for February and July.

DIC and TA variability is highly dependent on the tidal coefficient, and proportional to salinity tidal amplitude. Tidal amplitude ranges from 286 to 278 $\mu\text{mol kg}^{-1}$ and from 604 to 746 $\mu\text{mol kg}^{-1}$ for TA and DIC values, respectively. The minimum pH is generally observed at low tide and maximum at high tide, although this pattern is more scattered for February and May. In order to facilitate discussion of the dissolved oxygen variability, the AOU has been used as the parameter accounting for the balance between respiration and primary production in the surface water, the AOU being positive when respiration exceeds primary production. For most of the samplings, the AOU maximum is in the early morning and it decreases to a minimum in the hours of maximum solar irradiation and temperature (around 15:00 h GMT); this finding is in good agreement with biological processes (balance production–respiration), unlike the behaviour of TA and DIC which seems to be linked to water level variations. The chlorophyll tidal pattern is very scattered for most of the tidal samplings, and no pattern associated with water level has been observed.

In order to study the conservative behaviour of the different physicochemical properties, the TA, DIC, Chl-*a* and AOU have been plotted versus salinity, to determine whether or not they follow a linear relationship. The results of the tidal sampling for spring and neap tides are shown in Fig. 5. The TA displays a conservative

behaviour for most of the tidal sampling performed, and there is a good correlation versus salinity (the r^2 ranges between 0.81 and 0.98). Similarly, DIC presents a good linear fit versus salinity (with the r^2 ranging between 0.75 and 0.97). For both TA and DIC, the slope of their fit versus salinity changes from negative in winter–spring to positive in summer–autumn due to the inversion in the salinity gradient in the tidal creek; however, over the full year, the maximum DIC and TA occur at low tide and hence in the innermost part of the creek. For the samplings carried out on 1 March and 4 May, which are considerably affected by runoff, the r^2 drops to 0.4 and 0.2 for TA and DIC, respectively, because of the inputs from land drainage. For the remaining dates, and especially for DIC and TA, the system could be described as two component endmembers whose mixing explains almost all the daily variability. The differences in TA and DIC between day and night (February and March, Fig. 4) are proportional to salinity differences; this suggests that the influence of the daily biological cycle on TA and DIC is low. In the case of the Chl-*a* and AOU, unlike inorganic carbon, for cases, no conservative pattern is observed.

Besides water mixing and advection, organic matter respiration in the water column (Cai and Wang, 1998) and benthic fluxes (Forja et al., 2004) are other mechanisms capable of influencing the tidal variability of inorganic carbon. Other authors emphasise

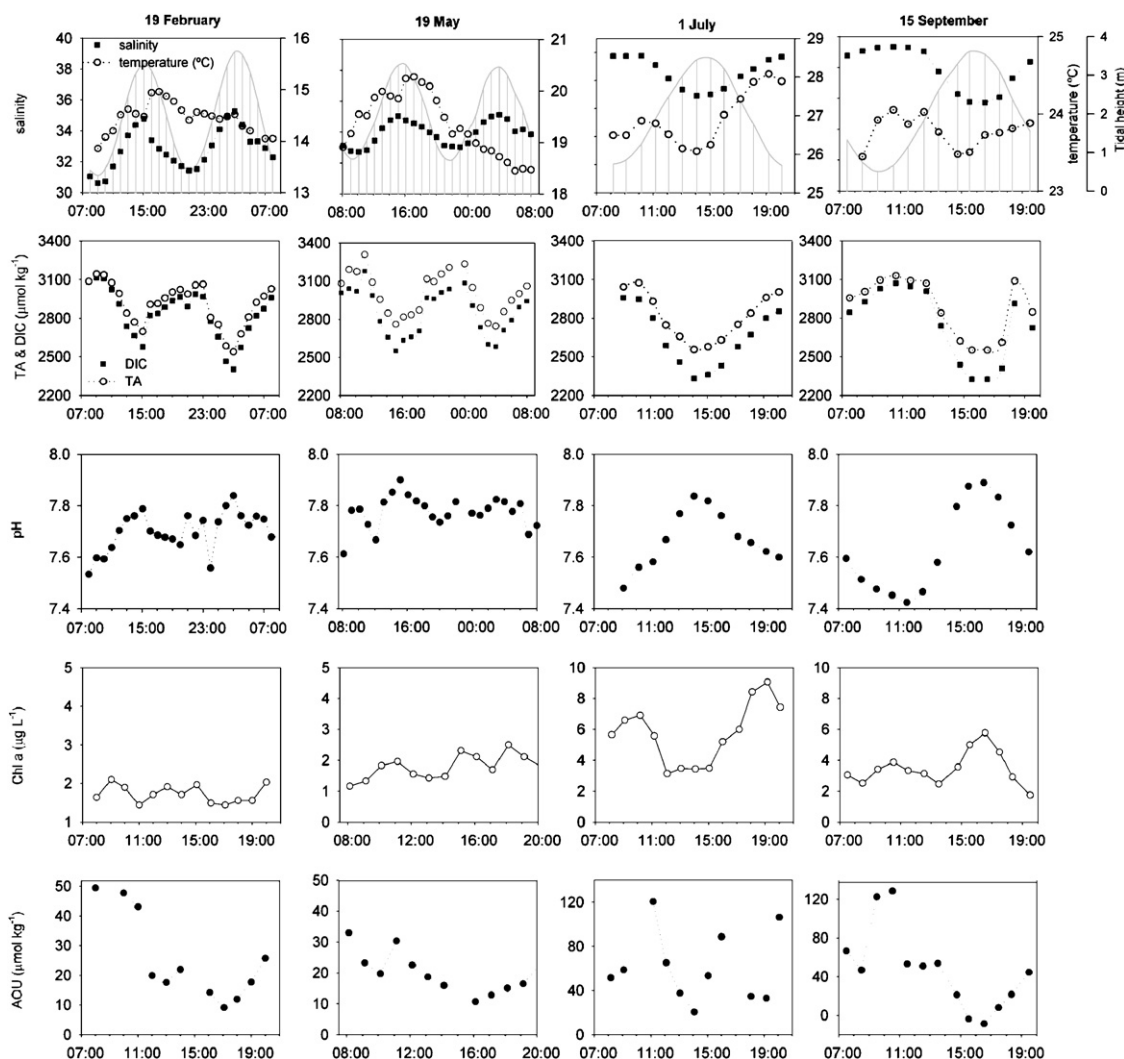


Fig. 4. Tidal variability of salinity, total alkalinity (TA), dissolved inorganic carbon (DIC), pH, Chlorophyll-*a* (Chl-*a*) and apparent oxygen utilisation (AOU) for four of the sampling dates. Tidal height is marked by the grey area. Most of the samplings are at spring tide, except one intermediate tidal coefficient on 19 May.

the relevance of lateral inputs of organic and inorganic carbon originating from the adjacent marshes via drainage and diffusion as the mechanisms that maintain the high respiratory rates usually found in salt marsh systems (Neubauer and Anderson, 2003; Wang and Cai, 2004). In the case studied here, however, the impact on the Rio San Pedro from the salt marshes has been largely reduced by human impact, except for the inputs derived from on-land run-off in rainy periods.

The Chl-*a* values exhibit high daily variability, but do not follow any reproducible tidal pattern nor theoretical dilution line. The reason for this could be that the biomass of primary producers is usually quite patchy in this system related to a complex combination of factors including light availability, concentration of nutrients and tidal resuspension of microphytobenthos. It is possible that there is a spatial maximum Chl-*a* value, the location of which is a function of the balance between turbidity and nutrient availability, and that this maximum position is displaced with tidal movements in and out of the creek. This phenomenon has been previously described for other systems such as a Brazilian estuary (Pereira-Filho et al., 2001).

On a longer time scale, there is an evident spring–neap tidal cycle for most of the physicochemical properties as a function of the percentage of water renewal (see Table 1). Water renewal has been calculated using the tidal prism method (Dyer, 1997) based

on the tidal height chart provided by the Instituto Hidrográfico de la Marina. In this context, DIC and TA show similar maximum low tide values for different water renewal percentages, while the minimum daily values, linked to high tide, decrease in line with the degree of dilution from the entry of water from the Bay of Cadiz. Similarly, the daily pH maximum increases with the water renewal. Chl-*a* presents higher values for neap tide than for spring tide. The explanation for this could be that an increase in the residence time of the water inside the creek favours the growth of the phytoplankton biomass when there are high concentrations of nutrients. In other estuaries, the low residence time has been identified as the limiting factor for phytoplankton biomass growth, in spite of extremely high nutrient concentrations (Wang et al., 2004).

3.2.2. Seasonal variability

In order to assess the seasonal variability of the physicochemical properties and their controlling mechanism, the tidal average for DIC, salinity, pH, AOU and Chl-*a* has been calculated for all the tidal samplings performed during 2004 (Fig. 6). The seasonal pattern for salinity shows the precipitation–evaporation annual cycle, with minimum salinity observed in February, corresponding to a precipitation rate of 761 mm month⁻¹, followed by May, when

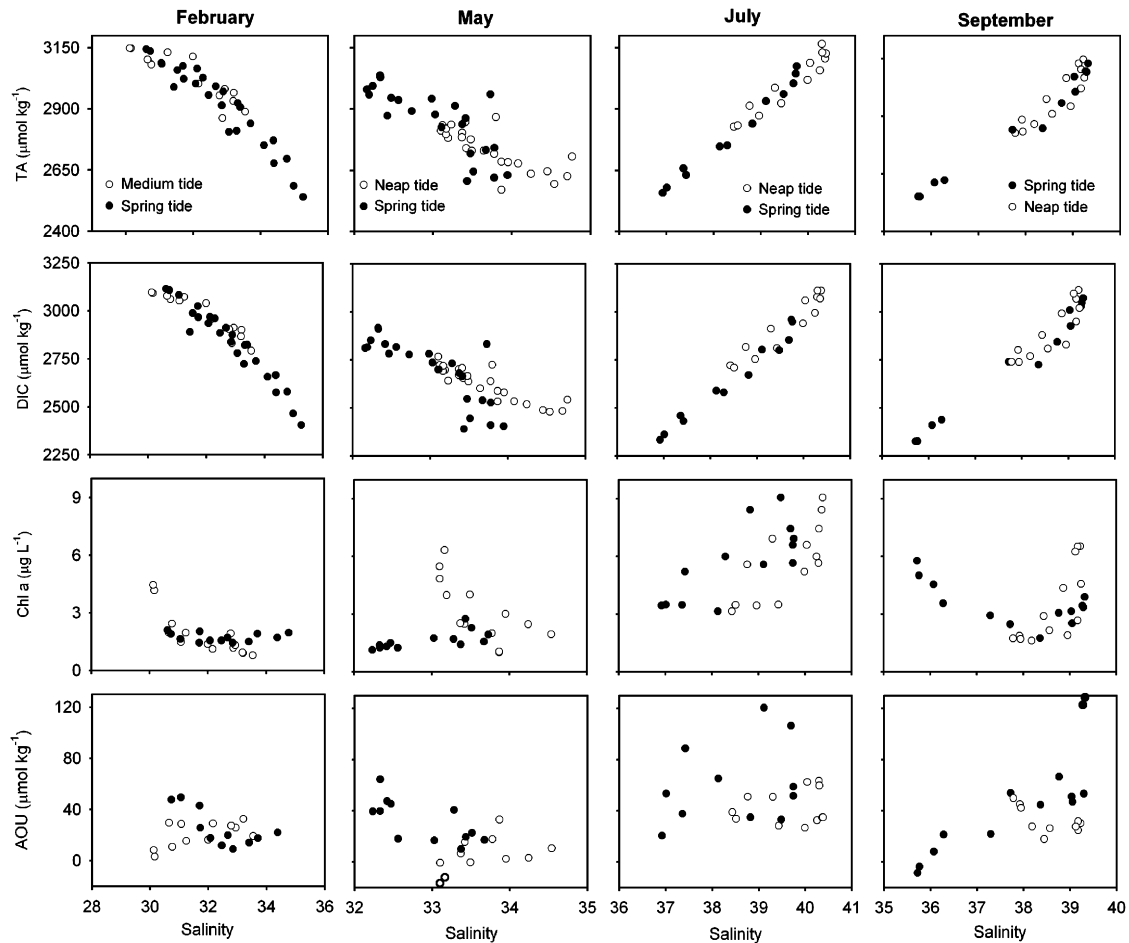


Fig. 5. Total alkalinity (TA), dissolved inorganic carbon (DIC), Chlorophyll-*a* (Chl-*a*) and apparent oxygen utilisation (AOU) versus salinity at spring and neap tides.

a severe storm event occurred on 2 May (559 mm of precipitation), and a maximum salinity observed in July, when the precipitation was negligible. The annual precipitation in 2004 was 3802 mm, hence the period between February and May accounted for 56% of the annual precipitation. The annual maximum occurred in October (1055 mm month⁻¹), unfortunately not coinciding with our sampling period.

The seasonal amplitude in DIC variability is 186 $\mu\text{mol kg}^{-1}$, with the minimum observed in May and the maximum in February. The pH values range between 7.77 and 7.56 with the maximum reached in May and the minimum in July and September. Regarding the AOU and Chl-*a* values, a similar pattern is observed for both parameters, with minimum and maximum in February and July, respectively. Different controlling mechanisms for DIC and pH, on the one hand, and AOU and Chl-*a*, on the other, explain the differences in the seasonal pattern.

Surprisingly, the maximum DIC values are observed in February, when fish farm activities are considerably reduced. Hence, this maximum is better explained by the land drainage inputs from the surrounded salt marshes and the soil washed out during storm events. This is accompanied by a relative decrease in pH due to the acidic character of the rainwater drainage. In summer and autumn, the degradation of organic matter together with intensified fish farm production would cause an increase in the TA and DIC concentration, in addition to a significant decrease in pH.

The positive value of the AOU over the full year indicates that respiratory processes of the organic matter exceed those of photosynthesis. Its seasonal variability will be related to the

seasonality in the organic matter concentration in the system, in addition to the temperature dependence of the metabolic rates, which explain the progressive increase in AOU values towards their maximum in summer. The seasonal evolution of Chl-*a* will be determined by the availability of nutrients. However, following the observation by Tovar et al. (2000a), the seasonal pattern of nutrients in the Rio San Pedro is different from the known seasonal pattern for coastal waters, which is a function of factors such as phytoplankton consumption, temperature and availability of light. In the area under study, the increase in the nutrient concentration generally took place in summer, and highest concentrations are found in the autumn. Then there is a decrease in winter, with the minimum nutrient concentrations being found in springs. This seasonal pattern follows the growth rate curve of the fish cultivated on the farm (Tovar et al., 2000b). Therefore, the Chl-*a* value will follow this trend, with some exceptions, such as that observed on 1 March, when a Chl-*a* peak occurred (up to 14 $\mu\text{g L}^{-1}$), in response to high nutrient inputs, mainly nitrites and nitrates (nutrient data provided by the *Delegacion de Medio Ambiente de la Junta de Andalucia*) and to the favourable conditions caused by the high residence time for that date (see Fig. 6, February neap tide).

Therefore, several interrelated processes are involved in the seasonality of the inorganic carbon system and related physico-chemical parameter such as AOU and Chl-*a*. Firstly, the high seasonality in the material inputs to the Rio San Pedro (mainly nutrients, organic matter and SPM) originating from the fish farm discharges. This is supported by the results founded by Tovar et al. (2000b), who studied the seasonality in the outflows from the fish

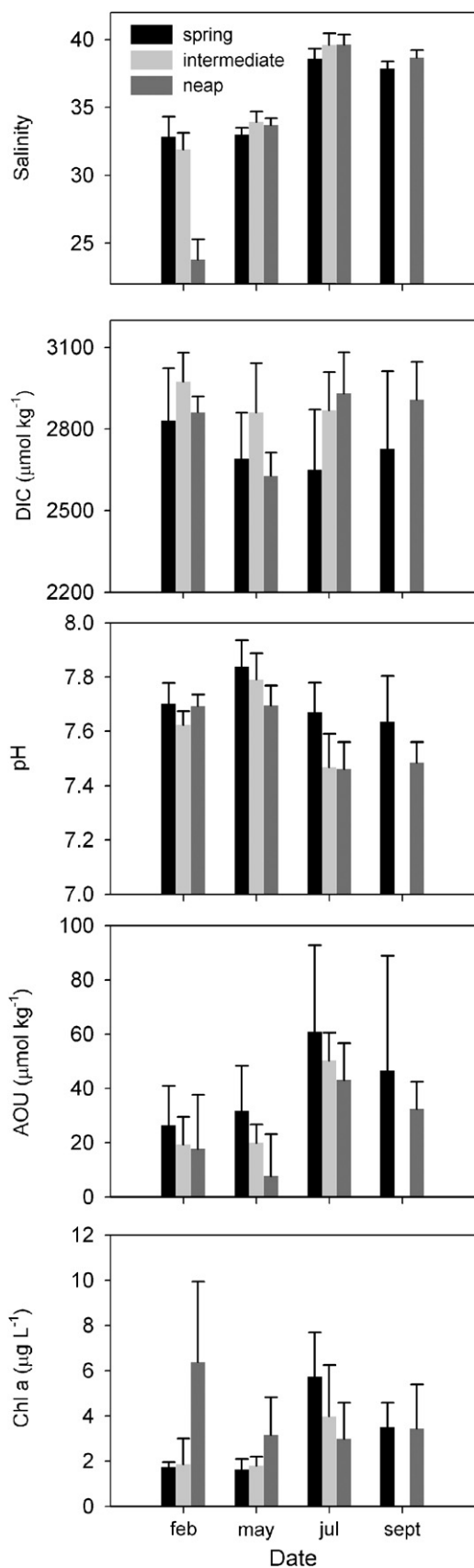


Fig. 6. Seasonal evolution of salinity, dissolved inorganic carbon (DIC), Chlorophyll-*a* (Chl-*a*), apparent oxygen utilisation (AOU) and pH.

farm over 2-year period. An increase was found in the fish production cycle with the temperature, with maxima in summer and autumn, and consequently the maximum discharge of nutrients, dissolved organic carbon and particulate material to the tidal creek.

Secondly, metabolic rates increase with temperature in the water column, as well as in the benthic compartment. In this context, the positive values of the AOU indicate that respiratory processes exceed production activities in the tidal creek (including water column and sediment).

A temperature increase from May to July slightly higher than 8 °C leads to an increase in the AOU value of 160% and 90% for Chl-*a*. It can be observed that the oxygen consumed is highly dependent on temperature as a consequence of the increasing magnitude of the respiratory processes with the temperature. Likewise, Chl-*a* values also show a high seasonal temperature dependence.

This seasonal temperature dependence has been described for other salt marsh systems that have not been altered by human activities. For instance, in the Duplin river, the salt marsh respiration increases the release of organic and inorganic carbon in summer and autumn, and lower rates are found in winter and spring (Wang and Cai, 2004). Similar features are found for other tidal estuarine freshwater marshes (Neubauer and Anderson, 2003) and the waters adjacent to salt marshes like the US South Atlantic Bight (Cai et al., 2003).

3.3. Inorganic carbon export to the adjacent coastal waters

The Rio San Pedro is a tidal creek where the only seawater input is by tidal exchange, and the only freshwater sources, mainly at the headwaters, are ultimately rainfall and inland drainage. The most predictable mechanism for flushing a small, well-mixed system is the regular rise and fall of water of the tide, but a number of other factors can also affect the flushing, for instance precipitation and land drainage inputs; none of these however have a significant value relative to the tidal prism, nor are they as predictable as the astronomical tides. In the present study, the classical tidal prism model has been used in order to assess the DIC export to adjacent coastal water. For this model, over each tidal cycle a volume of water (P) outside the tidal creek (i.e. in the Bay of Cadiz), with a DIC concentration of “DIC_B” enters the channel during the flood tide; it then mixes with the water of the creek with a volume V and a DIC concentration of “DIC_C” which dilutes after the mixing to a lower DIC concentration of DIC_T; later a volume equal to the tidal prism that entered (P) and with a final concentration of DIC_T, leaves the creek during the ebb. Then the mixing with ambient water outside the creek dilutes the tidal exported water to a concentration of DIC_B. The dilution processes in the Bay are highly favoured due to the disproportionately larger volume of the Bay of Cadiz in comparison to the Rio San Pedro, and to the circulation scheme of water in the Bay, where strong northward currents have been described near the mouth of the creek (Parrado et al., 1996); such circumstances tend to prevent any return flow into the creek after a tidal cycle.

The equivalent tidal mass DIC flux out of the tidal creek can be calculated from a modified version of the formula proposed by Sanford et al. (1992):

$$F = Q(\text{DIC}_T - \text{DIC}_B),$$

where F is the DIC tidal flux and Q is the volume flow rate. The value of Q can be calculated as the ratio between the tidal prism volume (P) and the tidal period (T) ($Q = P/T$). The tidal prism volume is defined as the water volume between low tide and high tide, and V is the water volume at low tide. Information must be available on the geometry of the channel and tidal elevations. The

dimensions of this channel have been approximated to a constant width of 110 m, a datum depth of 3 m, and a length of 12 km. The heights at low and high tide have been obtained from the 2004 tide table provided by the Instituto Hidrográfico de la Marina. The theoretical average DIC concentration, C_T , can be calculated from the DIC concentrations at both ends of the channel, and formulated as:

$$C_T = \frac{DIC_B P + DIC_C V}{P + V}.$$

To apply the tidal prism method, it is necessary to make some assumptions: firstly, that the DIC in the creek presents a conservative behaviour: this assumption can reasonably be accepted observing the theoretical dilution line of DIC (Fig. 5) which shows that mixing is the key factor controlling DIC variability on a tidal scale. Secondly, since the DIC_B value has not been measured for every sampling, it has been assumed that the DIC concentration in the Bay is equal to the most diluted experimental DIC value measured at our sampling station, corresponding to high water concentration at spring tide. This assumption has been tested satisfactorily with the salinity and with the DIC for various data available inside and outside the tidal creek in July 2003. DIC concentrations in the Bay of Cadiz were previously described in Section 3.1.

The DIC_C value for the innermost end of the creek is the maximum DIC concentration reached for each month, which is highly reproducible for the samplings carried out in the same period of the year, besides the tidal coefficient, with some exceptions observed during high rainfall events, as is the case on 1 March and 4 May. For these exception dates, C_T has been approximated to the average concentration measured over the tidal cycle at the tidal sampling station. The data for DIC concentrations have been multiplied by the water density in order to obtain the appropriate units (mol m^{-3}) for the DIC export calculation.

In order to check the consistency of the water budgets, the salinity data have been used to test the values obtained for V and P , as well as the applicability of the tidal prism model to the Rio San Pedro. The maximum difference between real and estimated values for salinity is around 1%, which is considerably less than the salinity range over a tidal cycle. Similarly, a comparison has been made between the average DIC concentration in a tidal cycle and the DIC_T resulting from the application of the tidal prism model. The average difference found between them is 3.5%, indicating that the tidal prism model, despite its simplicity, is a good approach for the DIC export calculation in the Rio San Pedro. Nevertheless, the DIC export found in this study may be overestimate because, firstly, the tidal creek presents an internal DIC longitudinal gradient that would affect the C_T estimation; and secondly, although it has been assumed that the return flow into

the creek after the tidal cycle is negligible (based on the available literature on the hydrodynamics of the Bay of Cadiz), this assumption could lead to a slight underestimation of C_B .

Table 2 shows the resulting DIC export calculated, together with other parameters required for the export calculations. It can be observed how the DIC export is a combination of the water flow (Q) and hence the tidal coefficient, as well as the DIC concentration gradient between the Rio San Pedro tidal creek and the Bay of Cadiz. The maximum DIC export, $43.7 \times 10^5 \text{ mol C d}^{-1}$, is obtained on 1 July, coinciding with spring tide, and the minimum export, $9.9 \times 10^5 \text{ mol C d}^{-1}$, on 27 April corresponding to neap tides and a higher DIC concentration in the Bay. To measure the relative effects of rain and water drainage on the water flux rate, a longer salinity record available for the study site has been analysed. The freshwater inputs have been determined as the water volume needed to dilute the average salinity with respect to a non-rainy initial situation for each month. This calculation yields an additional flow to Q of $0.2 \times 10^6 \text{ m}^3 \text{ d}^{-1}$ for 1 March (which is 11 times lower than the tidal flow for this date), and the net DIC export would increase from 9.9×10^5 to $10.8 \times 10^5 \text{ mol C d}^{-1}$. Nevertheless, the additional freshwater volume for 4 May is negligible compared to the tidal prism since the rainfall event coincides with a spring tide. In any case, it is also likely that the volume contributed by rainfall inputs, as well as by water drainage, would be relatively negligible compared to the tidal prism volume, and would thus have little effect on the water fluxes. The main effect due to these wash-out inputs will be noted in the DIC concentration in the tidal creek, as can be appreciated in the theoretical dilution line in Fig. 5, especially on 1 March and 4 May, when some deviation of DIC values from the expected linear dilution line are observed.

Seasonal variability of the DIC tidal export and the DIC concentrations in the innermost part of the creek follows the same pattern. It is worth noting that the highest variability can be observed on the fortnightly scale, following the spring–neap tidal cycle. This can be appreciated in Fig. 7, which shows that there is a relatively good linear correlation between DIC export and tidal coefficient ($R^2 = 0.72$, if the 4 May result is not included), regardless of the season.

The net annual DIC export was estimated by averaging spring and neap tidal flux values for each season, which were then seasonally averaged, resulting in an annual DIC export of $8.72 \times 10^8 \text{ mol C yr}^{-1}$, equivalent to $1.05 \times 10^{10} \text{ g C yr}^{-1}$, with the maximum DIC export rates occurring in summer and autumn. The only previous study available on DIC tidal exchange in the area is the one conducted by Forja et al. (2003) in the Sancti Petri Channel in July 1999. Unlike the Rio San Pedro, this channel is connected at one end to the Atlantic Ocean and at the other end to the Bay of Cadiz. In turn, this channel is surrounded by intertidal marshes, and a complex network of secondary channels, in

Table 2
DIC export and the complementary parameters required for its calculation

Date	Tidal coefficient	DIC_B (mol m^{-3})	DIC_T (mol m^{-3})	Q ($10^6 \text{ m}^3 \text{ d}^{-1}$)	DIC export ($10^5 \text{ mol C d}^{-1}$)
16 February	0.63	2467	2961	4.2	20.6
19 February	0.94	2467	2862	7.1	28.1
01 March	0.37	2467	2912	2.2	9.9
27 April	0.32	2540	2783	2.3	5.6
04 May	1.05	2540	2746	8.8	18.1
19 May	0.75	2540	2964	6.5	27.7
01 July	0.89	2391	2766	6.8	43.7
12 July	0.49	2391	2998	3.4	27.4
26 July	0.55	2391	2954	4.0	30.7
07 September	0.27	2383	3021	2.4	15.1
15 September	0.97	2383	2796	7.9	32.7

Inorganic carbon in the Bay of Cadiz (DIC_B), tidal coefficient, inorganic carbon in the Rio San Pedro (DIC_T), tidal flow (Q), inorganic carbon export (DIC export).

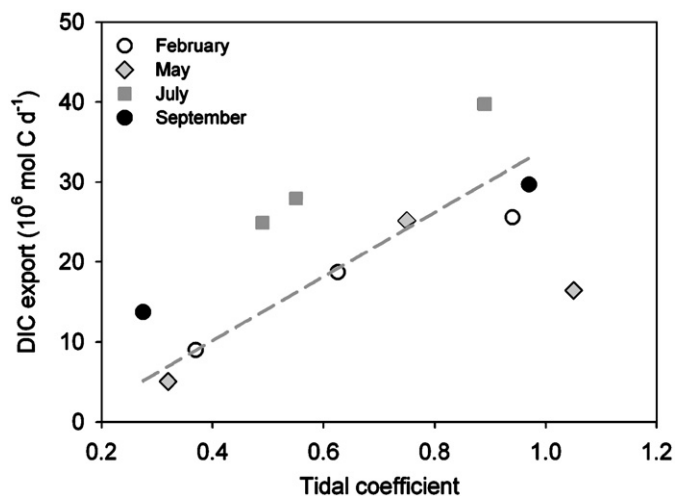


Fig. 7. Relationship between export of inorganic carbon and tidal coefficient.

addition to several fish farms and an urban waste water discharge point. These authors found a net export of DIC to the Bay of Cadiz of 10^{11} g C yr⁻¹, which is one order of magnitude higher than the resulting export from the Rio San Pedro. This higher export is explained by the higher net water flux and the greater area.

To gain a better understanding of the sources of this DIC exported, the DIC areal export has been calculated. The DIC export (1.05×10^{10} g C yr⁻¹) was then divided by the sum of the entire water surface area of the Rio San Pedro (1.85 km²) and the fish farm (1 km²), obtaining an estimation of 3673 g C m⁻² yr⁻¹ for the DIC areal export. This rate can be compared with other DIC sources. Due to the lack of information about the magnitude of the DIC export from the surrounding salt marshes to the tidal creek in our study area, we have analysed some data from the available literature corresponding to similar temperate ecosystems. Wang and Cai (2004) compiled some data available for the DIC export from salt marshes along the US south-eastern Atlantic continental shelf, and reported values ranging between 156 g C m⁻² yr⁻¹ in the Duplin River (a marsh-dominated non-riverine tidal river) up to 194 g C m⁻² yr⁻¹ for tidal freshwater marshes in Virginia. The DIC areal export from outside the Rio San Pedro is around 20 times higher than the DIC export from salt marshes described for other pristine systems, suggesting the existence of a significant source of DIC other than the surrounding salt marshes. Two principal sources of DIC to the Rio San Pedro water can be hypothesised: (a) DIC inputs from the fish farm discharge, probably remineralised in the sediment, due to the farm's high ratio of surface to volume; (b) organic matter respiration in the benthic and pelagic compartments inside the Rio San Pedro, principally of the organic material contained in the fish farm effluents. Taking into consideration the estimation by Tovar et al. (2000a), the mineralisation of the POM discharged by the fish farm inside the Rio San Pedro accounts for a small percentage (4%) of the estimated DIC export in this study, suggesting that the particulate inputs originating from the fish farm are not playing a significant role in the riverine DIC budget. The evaluation of the possible DIC sources must be treated with caution because the extent of output from a particular marsh area is related to specific factors such as geographic location, morphology and hydrology rather than to a universal feature of marshes (Boto and Wellington, 1988). Nevertheless, the disproportionate differences between the DIC export from salt marshes and the DIC areal export observed in the Rio San Pedro support the hypothesis about another non-natural (human induced) source and the impact of the fish farm. In turn, the Rio San Pedro is well-isolated from the surrounding salt

marshes, which suggests that the influence of the salt marsh on the Rio San Pedro is only moderate compared to similar systems, for instance the US south-eastern Atlantic coast.

Recently, García Lafuente and Ruiz (2007), carried out a review of the different mechanisms involved in the seasonal productivity in the Gulf of Cadiz, the continental shelf near the Rio San Pedro. They highlight the role of the Rio San Pedro and nearby waters as continuous sources of nutrients from land to the sea by means of tidal pumping. This permanent input of nutrients to the continental shelf favours the high productivity observed in the region under the influence of the Bay of Cadiz, in the primary and secondary trophic levels.

4. Conclusion

The results obtained in this study describe the temporal and spatial variability of the carbonate system in the Rio San Pedro, a tidal creek located within the Bay of Cadiz (SW Spain). Together with the measurement of DIC, Chl-*a* and AOU values contribute to assessing the main biological processes involved in the high temporal variability. Very high concentration gradients have been found between the Rio San Pedro and the Bay of Cadiz, which emphasise the role of the inner part of the tidal creek and the fish farm located at the head of the creek as intense sources of inorganic carbon to the system. Different mechanisms driving these processes have been found on different time scales. On a tidal scale, salinity has been revealed as a good tracker of tidal mixing, suggesting that TA and DIC present a nearly conservative behaviour. On a fortnightly time scale, there is a notable increase of the Chl-*a* values at neap tides, explained by an increase in the growth of the phytoplankton biomass with the residence time of the water inside the creek. Over the full year, there are two main factors explaining the seasonality of the inorganic carbon system and related parameters in Rio San Pedro tidal creek: the seasonality of the inputs (lateral inputs from marshes together with the production cycle of the fish farm effluents) and the seasonality of the metabolic rates. Furthermore, tidal creeks are extremely dynamic estuarine systems on a very short time scale as can be observed in the Rio San Pedro, where the magnitude of the seasonal amplitude of DIC is negligible compared with tidal and fortnightly time scales. The DIC tidal export from the Rio San Pedro to the Bay of Cadiz has also been calculated, and an annual average transport of 1.05×10^{10} g C yr⁻¹ has been obtained, with tidal pumping being the key mechanism. The dynamic nature of this system makes it necessary to obtain and analyse data on a variety of time-scales in order to present an accurate and realistic picture of the carbonate system in this coastal area.

Acknowledgements

This work was supported by the Spanish CICYT (Comisión Interministerial de Ciencias y Tecnología) of the Ministerio de Educación y Ciencia under contract CTM2005-01364/MAR. Thanks are expressed to CYCEM "El Toruño" for providing the infrastructures and to D. Gabriel for her assistance with the field work.

References

- Alongi, D.M., 2002. Present state and future of the world's mangrove forests. *Environmental Conservation* 29 (3), 331–349.
- APHA, 1992. American Public Health Association. Standard Methods for the Examination of Water and Wastewater. Washington, DC, 312pp.
- Benson, B.B., Krause, J.R., 1984. The concentration and isotopic fractionation of oxygen dissolved in freshwater and seawater in equilibrium with atmosphere. *Limnology and Oceanography* 29, 620–632.

- Boto, K.G., Wellington, J.T., 1988. Seasonal variations in concentrations and fluxes of dissolved organic and inorganic materials in a tropical, tidally-dominated, mangrove waterway. *Marine Ecology Progress Series* 50, 151–160.
- Cai, W.-J., Wang, Y., 1998. The chemistry, fluxes, and sources of carbon dioxide in the estuarine waters of the Satilla and Altamaha Rivers, Georgia. *Limnology and Oceanography* 43, 657–668.
- Cai, W.-J., Pomeroy, L.R., Moran, M.A., Wang, Y., 1999. Oxygen and carbon dioxide mass balance for the estuarine-intertidal marsh complex of five rivers in the southeastern US. *Limnology and Oceanography* 44 (3), 639–649.
- Cai, W.-J., Wang, Z.H.A., Wang, Y.C., 2003. The role of marsh-dominated heterotrophic continental margins in transport of CO₂ between the atmosphere, the land-sea interface and the ocean. *Geophysical Research Letters* 30 (16), 1849.
- Dickson, A.G., 1990. Standard potential of the reaction: $\text{AgCl(s)} + 1/2\text{H}_2(\text{g}) = \text{Ag(s)} + \text{HCl(aq)}$, and the standard acidity constant of the ion HSO_4^- in synthetic seawater from 273.15–318.15 K. *Journal of Chemical Thermodynamics* 22, 113–127.
- Dickson, A.G., Riley, J.P., 1979. The estimation of acid dissociation constants in seawater media from potentiometric titrations with strong base. I. The ionic product of water—KW. *Marine Chemistry* 7, 89–99.
- Dyer, K.R., 1997. *Estuaries: A Physical Introduction*, second ed. Wiley, London.
- Forja, J.M., Ortega, T., Ponce, R., de la Paz, M., Rubio, J.A., Gómez-Parra, A., 2003. Tidal transport of inorganic carbon and nutrients in a coastal salt marsh (Bay of Cádiz, SW Spain). *Ciencias Marinas* 29 (4), 469–481.
- Forja, J.M., Ortega, T., DelValls, T.A., Gómez-Parra, A., 2004. Benthic fluxes of inorganic carbon in shallow coastal ecosystems of the Iberian Peninsula. *Marine Chemistry* 85, 141–156.
- García Lafuente, J., Ruiz, J., 2007. The Gulf of Cadiz pelagic ecosystem: an overview. *Progress in Oceanography* 74 (2–3), 228–251.
- González-Gordillo, J.L., Arias, A.M., Rodríguez, A., Drake, P., 2003. Recruitment patterns of decapod crustacean megalopae in a shallow inlet (SW Spain) related to life history strategies. *Estuarine Coastal and Shelf Science* 56, 593–607.
- Körtzinger, A., Thomas, H., Schneider, B., Gronau, N., Mintrop, L., Duinker, J.C., 1996. At-sea intercomparison of two newly-designed underway pCO₂ systems—encouraging results. *Marine Chemistry* 52, 133–145.
- Lueker, T.J., Dickson, A.G., Keeling, C.D., 2000. Ocean pCO₂ calculated from dissolved inorganic carbon, alkalinity, and equations for K_1 and K_2 : validation based on laboratory measurements of CO₂ in gas and seawater at equilibrium. *Marine Chemistry* 90, 105–119.
- Meybeck, M., Ragu, A., 1995. *Water Quality of World River Basins*. UNEP GEMS Collaborating Centre for Fresh Water Quality Monitoring and Assessment, United Nations Environment Programme.
- Neubauer, S.C., Anderson, I.C., 2003. Transport of dissolved inorganic carbon from a tidal freshwater marsh to the York River estuary. *Limnology and Oceanography* 48, 299–307.
- Parrado, J.M., Gutierrez Mas, J.M., Achab, M., 1996. Determinación de direcciones de corrientes mediante el análisis de 'formas de fondo' en la Bahía de Cádiz. *Geogaceta* 20, 378–381.
- Pereira-Filho, J.C., Schettini, A.F., Rorig, L., Siegle, E., 2001. Intratidal variation and net transport of dissolved inorganic nutrients, POC and Chlorophyll *a* in the Camboriú River Estuary, Brazil. *Estuarine Coastal and Shelf Science* 53, 249–257.
- Rabouille, C., Mackenzie, F.T., Ver, L.M., 2001. Influence of the human perturbation of carbon, nitrogen, and oxygen biochemical cycles in the global coastal ocean. *Geochimica et Cosmochimica Acta* 65 (21), 3615–3641.
- Sanford, L.P., Boicourt, W.C., Rives, S.R., 1992. Model for estimating tidal flushing of small embayments. *ASCE Journal of Waterway, Port, Coastal and Ocean Engineering* 118 (6), 635–655.
- Smith, S.V., Hollibaugh, J.T., 1993. Coastal metabolism and the oceanic organic carbon balance. *Reviews of Geophysics* 31 (1), 75–89.
- Takahashi, T., Olafsson, J., Goddard, J.G., Chipman, D.W., Sutherland, S.C., 1993. Seasonal variation of CO₂ and nutrients in the high-latitude surface oceans: a comparative study. *Global Biogeochemical Cycles* 7 (4), 843–878.
- Tovar, A., Moreno, C., Manuel-Vez, M.P., García-Vargas, M., 2000a. Environmental impacts of intensive aquaculture in marine waters. *Water Research* 34, 334–342.
- Tovar, A., Moreno, C., Manuel-Vez, M.P., García-Vargas, M., 2000b. Environmental implications of intensive marine aquaculture in earthen ponds. *Marine Pollution Bulletin* 40, 981–988.
- Wang, Z.A., Cai, W.-J., 2004. Carbon dioxide degassing and inorganic carbon export from a marsh-dominated estuary (the Duplin River): a marsh CO₂ pump. *Limnology and Oceanography* 49 (2), 341–354.
- Wang, C.-F., Hsu, M.-H., Kuo, A.Y., 2004. Residence time of the Danshuei River estuary, Taiwan. *Estuarine, Coastal and Shelf Science* 60, 381–393.
- Zeebe, R.E., Wolf-Gladrow, D.A., 2001. *CO₂ in Seawater: Equilibrium, Kinetics, Isotopes*. Elsevier Sci., New York, 346pp.